LASER INTERFEROMETER GRAVITATIONAL WAVE OBSERVATORY
- LIGO -
CALIFORNIA INSTITUTE OF TECHNOLOGY
MASSACHUSETTS INSTITUTE OF TECHNOLOGY

Document Type	**LIGO-T040002-00-Z**	2004/01/14

The Signal-to-Noise Ratio as a Predictor of Detectability in the S1 Burst Search

Patrick J. Sutton

Distribution of this draft:

California Institute of Technology
LIGO Project - MS 51-33
Pasadena, CA 91125
Phone (626) 395-2129
Fax (626) 304-9834
E-mail: info@ligo.caltech.edu

Massachusetts Institute of Technology
LIGO Project - MS 20B-145
Cambridge, MA 01239
Phone (617) 253-4824
Fax (617) 253-7014
E-mail: info@ligo.mit.edu

WWW: http://www.ligo.caltech.edu/

Processed with LaTeX on 2004/01/14

Abstract

I compare common measurements of the size of simulated waveforms as a predictor of whether or not the signals would be detectable in the S1 analysis. I consider the signal-to-noise ratio ρ of optimal filtering, the peak amplitude $h_{\rm peak}$, and the root-sum-square amplitude $h_{\rm rss}$. These measures are applied to simulated Gaussian, sine-Gaussian, and Zwerger-Muller supernovae waveforms in the S1 data. Of these three measures, the S1 simulations indicate that the signal-to-noise ratio is the best predictor of the detectability of all three types of waveform considered. If this preliminary conclusion is borne out by further simulations with more types of waveforms, it motivates the adoption of the signal-to-noise ratio as a standard means for reporting the detection efficiency of the burst analysis.

Contents

1 Introduction

In the S1 bursts paper [1] the efficiency of the analysis pipeline for detecting gravitational-wave signals was presented for a total of nine ad-hoc waveforms: 2 Gaussians and 7 $Q \simeq 9$ sine-Gaussians.[1] The detectability of a given waveform was characterised primarily by the root-sum-square amplitude $h_{\rm rss}$ at which the triple-coincidence detection efficiency was 50%. For the sine-Gaussians this $h_{\rm rss}$ amplitude at which 50% efficiency was reached simply followed the underlying detector noise curve:

$$h_{\rm rss} \simeq \frac{[10, 20]}{\sqrt{S(f_0)}}\,, \tag{1}$$

where f_0 is the central frequency of the sine-Gaussian and $S(f_0)$ is the noise power spectrum at this central frequency (see Figure 1 of [1]). This simple relationship holds because these sine-Gaussians are narrow bandwidth ($\approx f_0/Q$), so the underlying noise floor can be treated as a constant, $S(f_0)$, for any given sine-Gaussian. This relationship is useful because it enables us to predict the amplitude at which $Q = 9$ sine-Gaussians with other central frequencies would be detectable.

[1] Detection efficiencies were also measured for 8 Zwerger-Muller waveforms, but these were not included in the S1 paper.

While $h_{\rm rss}$ is adequate for describing the efficiency of the S1 analysis pipeline for sine-Gaussians, it is not clear that it is adequate for more general waveforms, especially broadband waveforms. By definition a broadband waveform will have to compete with the noise over a large frequency range, so a simple relation like (1) cannot be expected to hold. This leaves us with the question of how to characterise the detectability of generic candidate signals. In the S1 paper this question was handled by tabulating the 50% efficiency amplitudes for the Gaussian and sine-Gaussian signals tested. This is unsatisfactory for two reasons:

1. In the S2 analysis it is expected that the waveform set for simulations may be expanded greatly, especially to include astrophysically motivated waveforms. For example, in addition to the 78 Zwerger-Muller supernova waveforms, Dimmelmeier *et al.* [3] have released a catalog of 26 additional waveforms, and Ott *et al.* [4] have recently released a catalog of 72 new supernova waveforms. Black-hole mergers or ringdowns may also be studied. As we measure efficiencies for more waveforms, and for more complicated waveforms it is desirable to have a more concise and intuitive means of displaying efficiencies than tables of amplitudes.

2. Tabulated lists of amplitudes don't tell us how to determine if our analysis pipeline would have been sensitive to a signal which does not fit into one of the waveform families we tested; an actual set of simulations would have to be performed. This makes our upper limits of little use to the source community. For our upper limits to be useful, we must have a means of extrapolating from the empirically determined efficiencies to predict the efficiencies for other types of waveforms.

A standard means in the literature for characterising the detactability of a signal is the signal-to-noise ratio (SNR) for optimal filtering [5]. The SNR is useful because it naturally accounts for colored (frequency-varying) detector noise. In this document I study the SNR as an alternative means of characterising the efficiency of the S1 bursts pipeline, and compare it to the peak and root-sum-square (RSS) amplitudes, which are two of the other measures commonly used in the bursts group. Unlike the peak or RSS amplitudes, I find that the SNR at which a waveform becomes detectable at 50% efficiency is a simple function of the characteristic frequency of the waveform which is common to all three types of waveform tested. While preliminary (due to the small number of waveforms and waveform types for which we have simulation data), this generic behaviour implies that we may be able to predict the efficiency of the bursts event trigger generators to wide classes of waveforms without extensive simulations. This could be especially useful to applying our computed upper limits to arbitrary new signal models "after the fact."

2 Signal Characteristics

2.1 Amplitude Measures

The signal-to-noise ratio ρ of optimal filtering for a signal $h(t)$ is [5]

$$\rho = \left[4 \int_0^\infty df \, \frac{|\tilde{h}(f)|^2}{S(f)} \right]^{1/2} . \tag{2}$$

Here $S_h(f)$ is the one-sided power spectral density of the detector noise, which is assumed to be Gaussian, and $\tilde{h}(f)$ is the Fourier transform of $h(t)$.

Real detector noise is not Gaussian, and we do not use optimal filtering in the bursts analysis. Nevertheless, ρ has several highly convenient properties. Specifically, it depends only on the signal waveform and the detector noise, and naturally accounts for the variation in power of each over frequency. The value of ρ for which a given analysis procedure has 50% efficiency is also a good indicator of how close to optimal the procedure is; for reference, optimal filtering of LIGO data in the inspiral search is done with SNR thresholds in the area of $\rho \simeq 5 - 10$ [6].

Two other measures of signal amplitude commonly used in the Burst Group are the root-sum square amplitude,

$$\begin{aligned} h_{\text{rss}} &= \left[\int_{-\infty}^{\infty} dt\, h^2(t)\right]^{1/2} \\ &= \left[2\int_{0}^{\infty} df\, |\tilde{h}(f)|^2\right]^{1/2} , \end{aligned} \tag{3}$$

and the peak amplitude,

$$h_{\text{peak}} = \max\left(|h(t)|\right) . \tag{4}$$

Note that these measures are independent of the detector noise.

2.2 Frequency Measures

It will be useful to specify a characteristic frequency for each waveform. We will use

$$f_{\text{c}} \equiv \frac{\int_0^\infty df\, f \frac{|\tilde{h}(f)|^2}{S(f)}}{\int_0^\infty df \frac{|\tilde{h}(f)|^2}{S(f)}} . \tag{5}$$

For studying h_{rss} and h_{peak}, which are independent of the detector noise $S(f)$, it is more natural to use (5) with $S(f) = 1$, which we denote by f_{w}:

$$f_{\text{w}} \equiv f_{\text{c}}|_{S(f)=1} = \frac{\int_0^\infty df\, f |\tilde{h}(f)|^2}{\int_0^\infty df\, |\tilde{h}(f)|^2} . \tag{6}$$

3 Testing Signal Measures

To investigate the usefulness of these various signal measures in understanding burst detection efficiencies, I evaluate them for the simulated waveforms tested in the S1 analysis (based on TF-Clusters) using representative S1 noise data.

3.1 Waveforms

Simulations with S1 data have been carried out using narrowband and broadband ad-hoc waveforms and broadband astrophysically motivated waveforms.

The ad-hoc waveforms tested were Gaussians,

$$h(t) = h_{\text{peak}} \exp\left(-\frac{(t-t_0)^2}{\tau^2}\right), \tag{7}$$

and sine-Gaussians,

$$h(t) = h_{\text{peak}} \sin(2\pi(t-t_0)f_0) \exp\left(-\frac{(t-t_0)^2}{\tau^2}\right) . \tag{8}$$

The sine-Gaussians used $\tau = 2/f_0$ ($Q \simeq 9$). The envelope peak time t_0 is irrelevant for our purposes.

Tables 1 and 2 list the parameters used for each waveform and the h_{rss} amplitudes at which the sky-direction and polarization-averaged triple-coincidence TFClusters detection efficiency was 50%; these are taken directly from the S1 bursts paper [1].

τ (ms)	1.0	2.5
h_{rss} $(10^{-19}\text{Hz}^{-1/2})$	10	82

Table 1: The Gaussian waveforms tested and the RSS amplitude at which each was detectable with 50% efficiency, averaged over sky position and signal polarization.

f_0 (Hz)	153	254	361	554	850	1304	2000
h_{rss} $(10^{-19}\text{Hz}^{-1/2})$	16	5.1	3.8	4.2	7.3	14	23

Table 2: The sine-Gaussian waveforms tested (with $\tau = 2/f_0$) and the RSS amplitude at which each was detectable with 50% efficiency, averaged over sky position and signal polarization.

The RSS amplitude can easily be converted to peak amplitude for use with (7), (8). For Gaussians use

$$h_{\text{rss}} = \left(\frac{\pi\tau^2}{2}\right)^{1/4} h_{\text{peak}} , \tag{9}$$

while for sine-Gaussians use

$$h_{\text{rss}} = \left(\frac{\pi}{2f_0^2}\right)^{1/4} h_{\text{peak}} . \tag{10}$$

For comparison with the astrophysical waveforms, which were tested for optimal position and orientation only, we want to remove the averaging over sky direction and signal polarization. The 50% efficiency amplitudes for the 1ms Gaussian and 361Hz, 554Hz sine-Gaussians increased by a factor of 2.97 to 3.24 when this averaging was done. When comparing to the astrophsycial waveforms, therefore, I compensate approximately by dividing the amplitudes for the ad-hoc waveforms by 3.

For astrophysical flavour, eight Zwerger-Muller supernova waveforms [2, 7] were also tested, though not included in the S1 paper. The specific waveforms and the distance at which each was detectable by TFClusters with 50% triple-coincidence efficiency (for optimal position and orientation) are listed in Table 3 [8].

waveform	A1B1G5	A1B3G1	A1B2G4	A2B4G2	A4B1G5	A4B5G5	A2B1G3	A1B2G2
d (pc)	0.5	12	3	10	4	40	7	30

Table 3: The Zwerger-Muller waveforms tested and the distance at which each was detectable with 50% efficiency for optimal position and orientation.

3.2 Procedure

The procedure for evaluating the various signal measures is as follows:

1. For each waveform, evaluate ρ, h_{rss}, h_{peak}, f_{c}, and f_{w} as in (2)–(6), using the 50% efficiency amplitudes implied by Tables 1-3.

   There are a couple of technical points in evaluating these measures.

   (a) In evaluating these measures using S1 data I restrict the frequency integrals to the interval [150,4000]Hz. The lower limit corresponds to the cut-off frequency of the high-pass filter applied to the data before it was passed to an event trigger generator. The upper limit is arbitrary, as none of the signals tested have significant power above approximately 2kHz.

   (b) For and concreteness, the noise spectrum $S(f)$ used is the envelope of the official representative S1 noise spectra for the three LIGO interferometers [9]; ie, at each frequency

   $$S(f) = \max(S_{\text{H1}}(f), S_{\text{H2}}(f), S_{\text{L1}}(f)) \,. \tag{11}$$

   Another possibility (which I did not investigate) is to evaluate ρ separately for each detector and select the largest ρ as the threshold for detection.

2. Plot each measure $X \in \{\rho, h_{\text{rss}}, h_{\text{peak}}\}$ versus characteristic frequency f_{c} or f_{w} for each waveform. A good measure X is one which is a good predictor of the 50% efficiency of any waveform:

   Ideal: $X(f)$ is a universal constant for all waveforms (ie, a flat line). This is ideal because we can predict that any given waveform is detectable with greater than 50% efficiency by evaluating X for it and comparing to this constant.

   Good: $X(f)$ is a smooth, sharply defined curve for all waveforms, preferably varying over only a small range. A waveform is detectable if the point (f, X) lies above this curve.

   Bad: $X(f)$ varies over a large range and shows waveform-dependent behaviour. We cannot use such a measure to predict whether a waveform will be detectable.

4 Performance

Plots of ρ vs. $f_{\rm c}$, $h_{\rm rss}$ vs. $f_{\rm w}$, and $h_{\rm peak}$ vs. $f_{\rm w}$ are shown in Figures 1, 2, 3.

The SNR appears to be a better efficiency predictor than the RSS or peak amplitude (though the RSS is not bad either). The range of variation in the SNR is the smallest at a factor of approximately 3.5, compared to factors of 22-23 for the RSS and peak amplitudes. Moreover, in terms of SNR the three waveform families all form a single, fairly well defined curve (the Zwerger-Mullers being the least well-behaved). When characterised by RSS or peak amplitude, the broadband and narrowband signals lie on separate curves.

The SNR has the least variation because it automatically accounts for the changing noise floor.

The sine-Gaussians follow a smooth curve in each measure; this is because of their narrowband nature. What is more interesting is that in each case the broadband signals also appear to fall along a fairly smooth, well-defined curve. That is, the Zwerger-Muller waveforms appear to share a common curve with the Gaussians, though it is impossible to be certain since only 2 Gaussian waveforms are tested. It may be that, for purposes of detection efficiency, the Zwerger-Mullers are equivalent to Gaussians of the same characteristic frequency.

The broadband RSS curve intersects the narrowband curve at the noise floor minimum (around 400Hz) but is above the narrowband curve where the noise is higher. This is probably due to the fact that the energy of broadband signals extends into regions of higher noise; this portion of the signal energy does not contribute significantly to the detectability of the signal. Hence, broadband signals near "walls" of the noise require a higher RSS than a narrowband signal of the same characteristic frequency to be detectable. This is automatically accounted for in the SNR.

The flatness or range of variation of the 50% efficiency curve will be especially important for signals for which the characteristic frequency is not phyiscally meaningful. A trivial example would be the sum of two sine-Gaussians of different central frequencies. If the 50% curve is flat, then errors in the assignment of a physical frequency are not important for determining if the signal will be detectable. (It would be interesting to see how these measures perform for such signals.)

Variations of the SNR curve also show where the analysis is performing closer to or farther from optimality. For example, the SNR curve of Figure 1 indicates that TFClusters was most sensitive to signals centered on 400Hz. This is consistent with the fact that in S1 TFClusters was tuned for maximum efficiency for signals with a bandwidth of 40Hz (five times the frequency resolution of 8Hz each) when the signal duration is much less than the TFClusters temporal resolution of 125ms; 40Hz is the approximate bandwith of a $Q \simeq 9$ sine-Gaussian with a central frequency of about 400Hz. The higher values of the threshold SNR at other frequencies imply that we could do better at these frequencies by running TFClusters with different optimal bandwidths (this is being done in the S2 analysis).

As an aside, note that the detection curves will be different for different event trigger generators. For example, the threshold curve for Slope in the S1 analysis has a minimum near 1kHz; this is expected from the tuning of Slope in S1 [1].

The absolute scale of the threshold SNR values is also consistent with (1). The apparent discrepancy is due to the fact that we are using the triple-coincidence 50% efficiencies, which are higher than the single-detector 50% efficiencies described by (1). For example, if the three detectors have the same noise level, then

$$h^{3\times}_{50\%} \simeq h^{1\times}_{80\%}\,, \tag{12}$$

whereas in the other extreme, when one detector has much higher noise than the others,

$$h^{3\times}_{50\%} \simeq h^{1\times|\mathrm{loudest}}_{50\%} \,. \tag{13}$$

From Figure 10 in the S1 paper [1] I estimate

$$h^{1\times}_{80\%} < 1.5 \times h^{1\times}_{50\%} \,. \tag{14}$$

We can expect that converting from single-detector efficiencies to triple-coincidence efficiencies thus raises the threshold amplitude by a factor $F^{3\times}$ in the approximate range [1,1.5]. Combining this factor with (1), (2), and (3) leads us to expect threshold SNRs for sine-Gaussians in the range

$$\begin{aligned}
\rho^{3\times} &\simeq \left[4\int_0^\infty df\, \frac{|\tilde{h}^{3\times}(f)|^2}{S(f)}\right]^{1/2} && (15)\\
&\simeq \sqrt{\frac{2}{S(f_0)}}\left[2\int_0^\infty df\, |\tilde{h}^{3\times}(f)|^2\right]^{1/2} && (16)\\
&\simeq \sqrt{\frac{2}{S(f_0)}}\, h^{3\times}_{\mathrm{rss}} && (17)\\
&\simeq \sqrt{2}F^{3\times}\frac{h^{3\times}_{\mathrm{rss}}}{\sqrt{S(f_0)}} && (18)\\
&\simeq \sqrt{2}\times[1,1.5]\times[10,20] && (19)\\
&\simeq [15,40]\,. && (20)
\end{aligned}$$

This is what we see in Figure 1.

5 Recommendation

This preliminary examination indicates that the signal-to-noise ratio as a function of signal characteristic frequency may be a powerful indicator of the bursts pipeline detection efficiency for broad classes of waveforms. This could provide a concise and intuitive means for summarizing the sensitivity of the bursts pipeline to the many types of waveforms that we use in simulations. More importantly, it could provide a natural means for applying burst upper limits to signal models for which detailed simulations have not been carried out (though detailed simulations are of course always preferable).

Further examination of the signal-to-noise ratio (and other signal characteristics) should be done for the widest possible range of simulated signals.

References

[1] B. Abbott *et al.*, "First upper limits from LIGO on gravitational wave bursts" [arXiv:gr-qc/0312056].

[2] T. Zwerger and E. Muller, "Dynamics and gravitational wave signature of axisymmetric rotational core collapse," Astron. Astrophys. **320**, 209 (1997).

[3] H. Dimmelmeier, J. A. Font and E. Muller, "Relativistic simulations of rotational core collapse. II. Collapse dynamics and gravitational radiation," Astron. Astrophys. **393**, 523 (2002). [arXiv:astro-ph/0204289].

[4] C. D. Ott, A. Burrows, E. Livne and R. Walder, "Gravitational waves from axisymmetric, rotational stellar core collapse," arXiv:astro-ph/0307472.

[5] C. Cutler and E. E. Flanagan, "Gravitational Waves From Merging Compact Binaries: How Accurately Can One Extract The Binary's Parameters From The Inspiral Wave Form?," Phys. Rev. D **49**, 2658 (1994) [arXiv:gr-qc/9402014].

[6] B. Abbott *et al.*, "Analysis of LIGO data for gravitational waves from binary neutron stars" [arXiv:gr-qc/0308069].

[7] The Zwerger-Muller catalog [2] and some discussion regarding it are available from the Burst Group's simulations catalog page,

`http://www.ligo.caltech.edu/~ajw/bursts/burstsim.html`

I used the waveforms supplied in the file "ZMcat.mat" available there. These waveforms are normalized for a supernova at 1 Mpc with optimal orientation (the waveforms have only one polarization).

[8] See

`http://emvogil-3.mit.edu/~cadonati/S2/PlaygroundFirstPass/index.html`

Note that the 50% triple-coincidence amplitudes quoted on this page do not include the average over sky directions and signal polarizations. This makes them about a factor of 3 lower than the amplitudes reported in the S1 paper. [1].

[9] The official representative LIGO noise curves for each science run can be found at

`http://ligo.caltech.edu/~lazz/distribution/LSC_Data`

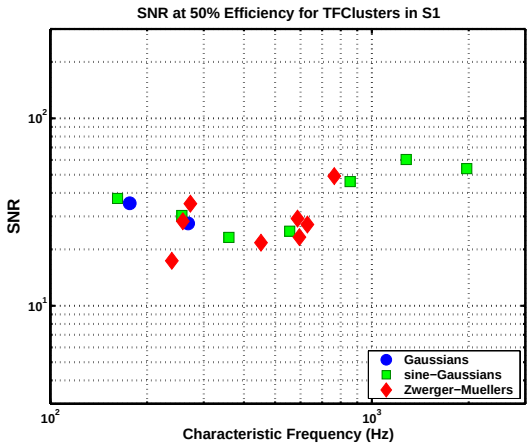

Figure 1: The signal-to-noise ratio ρ (2) at which various simulated waveforms have a 50% efficiency for detection versus the characteristic frequency f_c (5) of the waveform, for the S1 analysis.

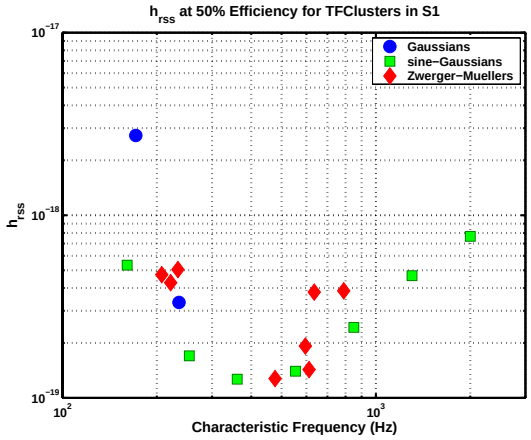

Figure 2: The root-sum-square amplitude $h_{\rm rss}$ (3) at which simulated waveforms have a 50% efficiency for detection versus the characteristic frequency $f_{\rm w}$ (6) of the waveform (without noise weighting), for the S1 analysis.

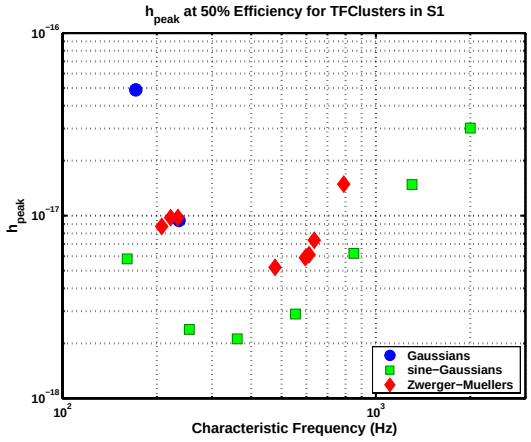

Figure 3: The peak amplitude $h_{\rm peak}$ (4) at which simulated waveforms have a 50% efficiency for detection versus the characteristic frequency $f_{\rm w}$ (6) of the waveform (without noise weighting), for the S1 analysis.